CrossMark

ORIGINAL PAPER

An improved car-following model considering the influence of optimal velocity for leading vehicle

Liu Fangxun · Cheng Rongjun · Ge Hongxia · Lo Siuming

Abstract In the paper, an improved car-following model based on the full velocity difference model considering the influence of optimal velocity for leading vehicle on a single-lane road is proposed. The linear stability condition of the model is obtained by applying the linear stability theory. Through nonlinear analysis, the time-dependent Ginzburg–Landau (TDGL) equation and the modified Korteweg–de Vries (mKdV) equation are derived to describe the traffic flow near the critical point. In addition, the connection between the TDGL and the mKdV equations is also given. Good agreement between the simulation and the theoretical results shows that the improved model can be enhanced the stability of traffic flow.

L. Fangxun · C. Rongjun (✉) · G. Hongxia
Faculty of Maritime and Transportation, Ningbo
University, Ningbo 315211, China
e-mail: chengrongjun@nbu.edu.cn

L. Fangxun · C. Rongjun · G. Hongxia
Jiangsu Province Collaborative Innovation Center for
Modern Urban Traffic Technologies, Nanjing 210096,
China

L. Fangxun · C. Rongjun · G. Hongxia
National Traffic Management Engineering and Technology
Research Centre Ningbo University Sub-centre,
Ningbo 315211, China

L. Siuming
Department of Civil and Architectural Engineering,
City University of Hong Kong, Kowloon 999077,
Hong Kong, China

1 Introduction

Now, traffic jam has been more and more popular in modern city and caused a lot of trouble to the majority of people. So, many traffic models such as hydrodynamic models [1–10], car-following models [11–13] and cellular automaton models [14] have been constructed to investigate various complex properties of traffic jams. In addition, several important achievements have been attained. Car-following models are a favorable type of microscopic traffic model describing the behavior of an individual driver [15]. At present, the widely used traffic models are improved car-following models [16–22].

In 1995, Bando et al. [23] proposed the optimal velocity model (for short, OVM) to describe the car-following behavior on a single-lane highway. But the OV model may appear too high acceleration and unrealistic deceleration. In order to overcome the deficiency, Helbing and Tilch [24] proposed a generalized force model (for short, GFM). But GFM cannot describe the delay time and the kinematic wave speed at jam density. Jiang et al. [25] presented the full velocity difference model (for short, FVDM) to solve the shortcoming in GFM. Because FVDM has too high deceleration, Ge et al. [26] proposed the two velocity difference model (for short, TVDM) by considering the ITS application.

Recently, some new car-following models were successively put forward to describe the traffic nature more realistically. Some of them were extended by introducing multiple headway or relative velocity information of car, and others considered the two factors at the same time [27–34].

As we all know, in the actual traffic, the most important factors that affect the behavior of the current vehicle are the influences of the leading vehicle. The car-following models mentioned above can reproduce many complex actual traffic phenomena, but most of these models were studied by considering the impact of the headway or velocity of the leading vehicle; for example, some models have been investigated by considering the impact of the headway of the leading vehicle [35], and others have been investigated by taking into account the velocity of the leading vehicle [36]. Our model is focused on the impact of the optimal velocity of the leading vehicle, which is rarely investigated. The results may be closer to the actual traffic and can make the traffic flow relatively stable. In view of this, the improved car-following model is presented to investigate the traffic flow.

Based on previous work, we will investigate an improved car-following model in this paper. In Sect. 2, the model is presented with considering full velocity difference and a new optimal velocity function, which is decided by the optimal velocity between the nth car and $n + 1$th car. The model is analyzed by using linear stability theory. In Sect. 3, the nonlinear analysis near the critical point for our model is made, so the TDGL equation and its corresponding soliton solution are obtained. In Sect. 4, the mKdV equation is derived. In Sect. 5, numerical simulation is given, and the conclusions are given in Sect. 6.

2 Car-following models and linear stability analysis

In 1995, Bando et al. [23] proposed the optimal velocity model (for short, OVM) to describe the car-following behavior on a single-lane highway. The motion equation is given as follows:

$$\frac{\mathrm{d}v_n(t)}{\mathrm{d}t} = a\left[V\left(\Delta x_n(t)\right) - v_n(t)\right], \quad (1)$$

where $v_n(t)$ is the position of car n at time t, $\Delta x_n(t) = x_{n+1}(t) - x_n(t)$ represents the headway of two suc-

cessive vehicles, a is the sensitiveness of a driver and $V\left(\Delta x_n(t)\right)$ is the optimal velocity function. The empirical data show that the OV model may appear too high acceleration and unrealistic deceleration.

In order to overcome the deficiency, Helbing and Tilch [24] proposed a generalized force model (for short, GFM), i.e.,

$$\frac{\mathrm{d}v_n(t)}{\mathrm{d}t} = a\left[V\left(\Delta x_n(t)\right) - v_n(t)\right]$$
$$+ \lambda H\left(-\Delta v_n(t)\right)\Delta v_n(t), \quad (2)$$

where H is the Heaviside function, λ is a sensitivity coefficient different from a, $\Delta v_n(t) = v_{n+1}(t) - v_n(t)$ is the velocity difference between the leading car $n + 1$ and the following car n. The simulation results show that the GFM is poor in the delay time of car motion and the kinematic wave speed at jam density.

In view of the problem, in 2001, Jiang et al. [25] presented the full velocity difference model (for short, FVDM) by introducing the positive relative velocity into the GFM to solve the shortcoming in GFM.

$$\frac{\mathrm{d}v_n(t)}{\mathrm{d}t} = a\left[V\left(\Delta x_n(t)\right) - v_n(t)\right] + \lambda\Delta v_n(t), \quad (3)$$

but the simulation results indicate that the FVDM has too high deceleration.

Ge et al. [26] presented a two-velocity difference (TVD) model that considers ITS application. The differential equation is as follows:

$$\frac{\mathrm{d}v_n(t)}{\mathrm{d}t} = a\left[V\left(\Delta x_n(t)\right) - v_n(t)\right]$$
$$+ \lambda G\left(\Delta v_n(t), \Delta v_{n+1}(t)\right), \quad (4)$$

where $G\left(\Delta v_n(t), \Delta v_{n+1}(t)\right) = p\Delta v_n(t) + (1 - p) \times \Delta v_{n+1}(t)$, and p denotes the weighting value. The results indicate that unrealistically high deceleration will not appear in the TVD model due to the consideration of ITS application.

Based on the above-mentioned models and because of the complexity of the actual traffic, drivers have to adjust their speed according to the complicated condition of traffic, to ensure traffic safety. In view of the above reasons, an improved car-following model considering the impact of the optimal velocity of the leading vehicle is presented, and we call it (OVLM, for short).

$$\frac{dv_n(t)}{dt} = a\left[V\left(\Delta x_n(t)\right) + \gamma\left(V\left(\Delta x_{n+1}(t)\right)\right.\right.$$
$$\left.\left. - V\left(\Delta x_n(t)\right)\right) - v_n(t)\right] + \lambda \Delta v_n(t), \quad (5)$$

where $\Delta v_n(t) = v_{n+1}(t) - v_n(t)$, and a is the sensitivity which corresponds to the inverse of the delay time τ, $\lambda\ (0 \leq \lambda \leq 1)$ and $\gamma\ (0 \leq \gamma \leq 1)$ is the weight coefficient, and the optimal velocity function is proposed by [16].

$$V\left(\Delta x_n(t)\right) = \frac{v_{\max}}{2}[\tanh\left(\Delta x_n(t) - h_c\right) + \tanh(h_c)], \quad (6)$$

where $\Delta x_n(t) = x_{n+1}(t) - x_n(t)$, h_c is the safety distance and $v_{\max}$ is the maximal velocity. The function $V(.)$ is a monotonically increasing function with an upper bound (maximal velocity) and has a turning point $\Delta x_n = h_c : V''(h_c) = 0$. Therefore, we can derive the TDGL equation from Eq. (5), which could describe traffic jams.

For later convenience of linear analysis, Eq. (5) can be rewritten as:

$$\frac{dx_n^2(t)}{dt^2} = a\left[V\left(\Delta x_n(t)\right) + \gamma\left(V(\Delta x_{n+1}(t))\right.\right.$$
$$\left.\left. - V\left(\Delta x_n(t)\right)\right) - \frac{dx_n(t)}{dt}\right]$$
$$+ \lambda\left[\frac{dx_{n+1}(t)}{dt} - \frac{dx_n(t)}{dt}\right]. \quad (7)$$

Further, Eq. (7) can be rewritten in terms of the headway:

$$\frac{d\Delta x_n^2(t)}{dt^2} = a\left[V\left(\Delta x_{n+1}(t)\right) - V\left(\Delta x_n(t)\right)\right.$$
$$+ \gamma\left[V\left(\Delta x_{n+2}(t)\right) - 2V\left(\Delta x_{n+1}(t)\right)\right.$$
$$\left.+ V\left(\Delta x_n(t)\right)\right] - \frac{d\Delta x_n(t)}{dt}\Big]$$
$$+ \lambda\left[\frac{d\Delta x_{n+1}(t)}{dt} - \frac{d\Delta x_n(t)}{dt}\right]. \quad (8)$$

Then, linear stability analysis can be conducted for OVLM. It is obvious that the traffic flow can reach the steady state when the vehicles run with constant headway h and constant velocity $V(h)$. Therefore, the steady-state solution is given as

$$x_n^0(t) = hn + V(h)t, \quad h = \frac{L}{N}, \quad (9)$$

where N is the total vehicle number and L is the road length.

Suppose $y_n(t)$ is a small deviation from the steady-state $x_n^0(t)$: $x_n(t) = x_n^0(t) + y_n(t)$. Substituting it into Eq. (7) and linearizing it yield

$$\frac{dy_n^2(t)}{dt^2} = a\left[V'(h)\Delta y_n(t) + \gamma\left(V'(h)\Delta y_{n+1}(t)\right.\right.$$
$$\left.\left. - V'(h)\Delta y_n(t)\right) - \frac{dy_n(t)}{dt}\right]$$
$$+ \lambda\left[\frac{dy_{n+1}(t)}{dt} - \frac{dy_n(t)}{dt}\right], \quad (10)$$

where $\Delta y_n(t) = y_{n+1}(t) - y_n(t)$ and $V'(h) = dV(\Delta x_n)/dt\ |\Delta x_n = h$.

Expanding $y_n(t) = \exp(ikn + zt)$, it reads

$$z^2 = a\left[V'\left(e^{ik} - 1\right) + \gamma V'\left(e^{ik} - 1\right)^2 - z\right]$$
$$+ \lambda z\left(e^{ik} - 1\right), \quad (11)$$

where $V' = V'(h)$. Let $z = z_1(ik) + z_2(ik)^2 + \ldots$; then, the first- and second-order terms of ik are:

$$z_1 = V'(h) \quad z_2 = \frac{1 + 2\gamma}{2}V'(h) - \frac{\left(V'(h)\right)^2 - \lambda V'(h)}{a}. \quad (12)$$

For small disturbances with long wavelengths, the uniform traffic flow is unstable in the condition that

$$a < \frac{2\left(V'(h) - \lambda\right)}{1 + 2\gamma}, \quad (13)$$

The stability condition is given:

$$a = \frac{2\left(V'(h) - \lambda\right)}{1 + 2\gamma}. \quad (14)$$

The result is relevant with the parameters γ, λ.

Figure 1 shows the phase diagram in the (h, a)-plane where h is the headway and a is the sensitivity. The neutral stability curves are indicated by the solid lines. The solid lines show the results of the neutral stability curves with different γ, λ. It shows the stable region, and the critical points increase with increasing the value of the parameter γ, λ.

As can be seen from the diagram (a) of Fig. 1, when $\gamma = 0, \lambda = 0$, the neutral stability line and the critical
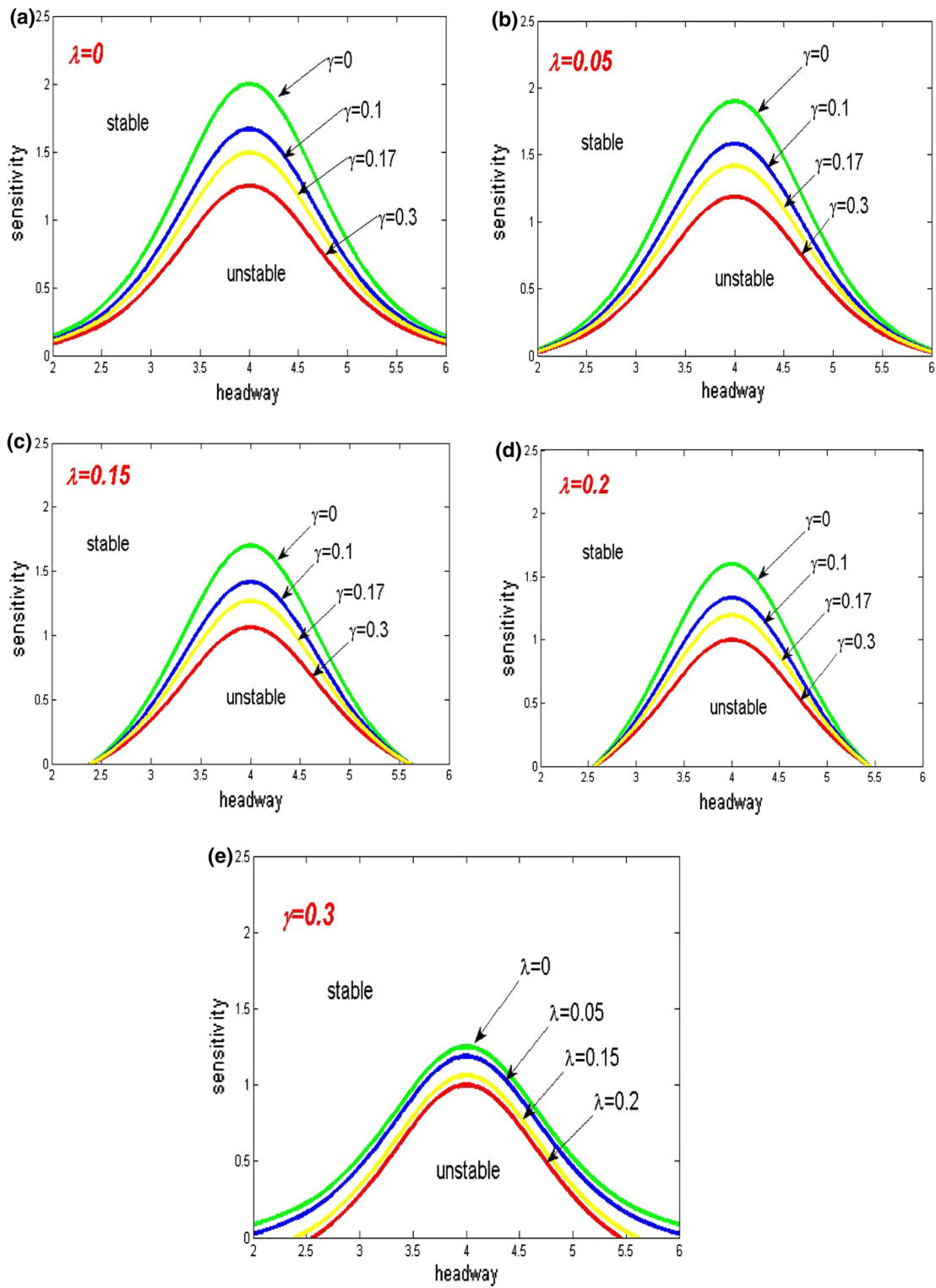
Fig. 1 Phase diagram of the model according to different values of parameter γ, λ from **a**–**e** ($v_{\max} = 2$, $h_c = 4$)

point in OVLM are consistent with those in OVM which proposed by Bando et al. Under the condition of traffic, it is very unstable.

As can be seen from the diagrams (a), (b), (c) and (d) of Fig. 1, when we fix λ [$\lambda = 0$ in diagram (a), $\lambda = 0.05$ in diagram (b), $\lambda = 0.15$ in diagram (c), $\lambda = 0.2$ in diagram (d)], increase γ ($\gamma = 0, 0.1, 0.17, 0.3$), the stable region will gradually increase, the traffic flow will become more stable.

From diagrams (a)–(d) of Fig. 1, when we take the same parameter γ in every diagram, with the gradual increase of λ from diagrams (a)–(d), regional stability will gradually increase, the traffic flow will be more stable. Obviously, from Fig. 1 we can see that OVLM is more stable than OVM.

In particular, from diagram (e) of Fig. 1, we can see that once comparing the four most stable curve of the four diagrams (a)–(d) of Fig. 1, the result shows that when the values are selected as $\gamma = 0.3, \lambda = 0.2$, the stable region reaches the best range.

3 TDGL equation

Now, we consider the traffic behavior of long-wavelength models on coarse-grained scales. The simplest way to describe the behavior of long-wavelength models is the long-wavelength expansion. The slowly vary behavior at long waves near the critical point is analyzed. The slow scales for space variable n and the time variable t are introduced, and the slow variables X and T are defined as follows:

$$X = \varepsilon (n + bt), \quad T = \varepsilon^3 t, \quad 0 < \varepsilon \le 1. \tag{15}$$

The headway $\Delta x_n(t)$ is set as

$$\Delta x_n(t) = h_c + \varepsilon R(X, T). \tag{16}$$

Substituting Eqs. (15)–(16) into Eq. (8) and expanding to the fifth order of ε, we obtain the following expression:

$$\varepsilon^2 \left(b - V' \right) \partial_X R + \varepsilon^3 \left(\tau b^2 - \frac{1 + 2\gamma}{2} V' - \tau \lambda b \right) \partial_X^2 R$$

$$+ \varepsilon^4 \left[\partial_T R - \left(\frac{\tau \lambda b}{2} + \frac{1 + 6\gamma}{6} V' \right) \partial_X^3 R \right.$$

$$\left. - \frac{V'''}{6} \partial_X R^3 \right] + \varepsilon^5 \left[\frac{1}{3} (2\tau b - \tau \lambda) \partial_X \partial_T R \right.$$

$$- \left(\frac{1 + 14\gamma}{24} V' + \frac{\tau \lambda b}{6} \right) \partial_X^4 R$$

$$+ \frac{1}{12} (1 + 2\gamma) V''' \partial_X^2 R^3 \right] = 0, \tag{17}$$

where $V' = V'(h_c) = \mathrm{d}V(\Delta x_n)/\mathrm{d}\Delta x_n |\Delta x_n = h_c$ and $V''' = V'''(h_c) = \mathrm{d}^3 V(\Delta x_n)/\mathrm{d}\Delta x_n^3 |\Delta x_n = h_c$

Now, we study the traffic flow near critical point $\tau = (1 + \varepsilon^2)\tau_c$. By taking $b = V'$, the second- and third-order terms of ε are eliminated from Eq. (17), which leads to the simplified equation as following:

$$\varepsilon^4 \partial_T R = \varepsilon^4 \left(\frac{\tau \lambda V'}{2} + \frac{1 + 6\gamma}{6} V' \right) \partial_X^3 R$$

$$- \varepsilon^4 \frac{|V'''|}{6} \partial_X R^3$$

$$+ \varepsilon^3 V' \left(\tau \lambda + \frac{1 + 2\gamma}{2} - \tau V' \right) \partial_X^2 R$$

$$- \varepsilon^5 \left[\tau (2V' - \lambda) \left(\frac{\lambda \tau V'}{2} + \frac{1 + 6\gamma}{6} V' \right) \right.$$

$$\left. - \frac{1 + 14\gamma}{24} V' - \frac{\tau \lambda}{6} V' \right] \partial_X^4 R$$

$$+ \varepsilon^5 \frac{|V'''|}{12} \frac{(1 + 2\gamma)(3V' - 2\lambda)}{V' - \lambda} \partial_X^2 R^3. \tag{18}$$

By transforming variables X and T into variables $x = \varepsilon^{-1} X$ and $t = \varepsilon^{-3} T$, and taking $S(x, t) = \varepsilon R(X, T)$, Eq. (18) is rewritten as follows:

$$\partial_t S = \left(\frac{\tau \lambda V'}{2} + \frac{1 + 6\gamma}{6} V' \right) \partial_x^3 S - \frac{|V'''|}{6} \partial_x S^3$$

$$+ V' \left(\tau \lambda + \frac{1 + 2\gamma}{2} - \tau V' \right) \partial_x^2 S$$

$$- \left[\tau (2V' - \lambda) \left(\frac{\lambda \tau V'}{2} + \frac{1 + 6\gamma}{6} V' \right) \right.$$

$$\left. - \frac{1 + 14\gamma}{24} V' - \frac{\tau \lambda}{6} V' \right] \partial_x^4 S$$

$$+ \frac{|V'''|}{12} \frac{(1 + 2\gamma)(3V' - 2\lambda)}{V' - \lambda} \partial_x^2 S^3. \tag{19}$$

By adding term $\frac{2V'(V' - \lambda)(\tau \lambda + \frac{1+2\gamma}{2} - \tau V')}{(1+2\gamma)(3V' - 2\lambda)} \partial_x S$ on both left and right sides of Eq. (19) and performing $t_1 = t$ and $x_1 = x - \frac{2V'(V' - \lambda)(\tau \lambda + \frac{1+2\gamma}{2} - \tau V')}{(1+2\gamma)(3V' - 2\lambda)} t$ for Eq. (19), we get

$$\partial_{t_1} S = \left(\partial_{x_1} - \frac{(1 + 2\gamma)(3V' - 2\lambda)}{2(V' - \lambda)} \partial_{x_1}^2 \right)$$

$$\left[\left(\frac{\tau \lambda V'}{2} + \frac{1 + 6\gamma}{6} V' \right) \partial_{x_1}^2 S \right.$$

$$- \frac{2V'(V' - \lambda)\left(\tau\lambda + \frac{1+2\gamma}{2} - \tau V'\right)}{(1+2\gamma)(3V' - 2\lambda)}S$$
$$\left. - \frac{|V'''|}{6}S^3\right]. \tag{20}$$

We define the thermodynamic potentials [37–40]:

$$\phi(S) \equiv -\frac{V'\left(V' - \lambda\right)\left(\tau\lambda + \frac{1+2\gamma}{2} - \tau V'\right)}{(1+2\gamma)\left(3V' - 2\lambda\right)}S^2$$
$$+ \frac{|V'''|}{24}S^4, \tag{21}$$

By rewritten Eq. (20) with Eq. (21), the TDGL equation is derived

$$\partial_{t_1}S = -\left(\partial_{x_1} - \frac{(1+2\gamma)(3V' - 2\lambda)}{2(V' - \lambda)}\partial_{x_1}^2\right)\frac{\delta\Phi(S)}{\delta S}. \tag{22}$$

With

$$\Phi(S) \equiv \int dx_1 \left[\frac{1}{2}\left(\frac{\tau\lambda V'}{2} + \frac{1+6\gamma}{6}V'\right)\left(\partial_{x_1}S\right)^2 + \phi(S)\right], \tag{23}$$

where $\delta\Phi(S)/\delta S$ indicates the function derivative. The TDGL Eq. (22) has two steady-state solutions except trivial solution S=0: One is the uniform solution:

$$S(x_1, t_1) = \pm\left[\frac{12V'(V' - \lambda)\left(\tau\lambda + \frac{1+2\gamma}{2} - \tau V'\right)}{(1+2\gamma)(3V' - 2\lambda)|V'''|}\right]^{\frac{1}{2}}, \tag{24}$$

And the other is the kink solution

$$S(x_1, t_1) = \pm\left[\frac{12V'\left(V' - \lambda\right)\left(\tau\lambda + \frac{1+2\gamma}{2} - \tau V'\right)}{(1+2\gamma)\left(3V' - 2\lambda\right)|V'''|}\right]^{\frac{1}{2}}$$
$$\times \tanh\left\{\left[\frac{12\tau V' - 12\tau\lambda - 6(1+2\gamma)}{6\tau\lambda + 2(1+6\gamma)}\right]^{\frac{1}{2}}\right.$$
$$\times \left.(x_1 - x_0)\right\}, \tag{25}$$

where x_0 is constant. Equation (25) represents the coexisting phase.

By the condition

$$\partial\phi/\partial S = 0, \quad \partial^2\phi/\partial S^2 > 0. \tag{26}$$

We obtain the coexisting curve from Eq. (21) in terms of the original parameters

$$(\Delta x)_{\mathrm{co}} = h_c \pm \left[\frac{12V'(V' - \lambda)\left(\tau\lambda + \frac{1+2\gamma}{2} - \tau V'\right)}{(1+2\gamma)(3V' - 2\lambda)|V'''|}\right]^{\frac{1}{2}}. \tag{27}$$

The spinodal line is given by the condition

$$\partial^2\phi/\partial S^2 = 0. \tag{28}$$

From Eq. (21), we obtain the spinodal line described by the following equation

$$(\Delta x)_{\mathrm{sp}} = h_c \pm \left[\frac{4V'(V' - \lambda)\left(\tau\lambda + \frac{1+2\gamma}{2} - \tau V'\right)}{(1+2\gamma)(3V' - 2\lambda)|V'''|}\right]^{\frac{1}{2}}. \tag{29}$$

The critical point is given by the condition $\partial\phi/\partial S = 0$ and Eq. (28).

$$(\Delta x)_c = h_c, \quad a_c = \frac{2\left(V'(h) - \lambda\right)}{1+2\gamma}. \tag{30}$$

4 mKdV equation

Similarly, we consider the slowly varying behavior at long wavelengths near critical point. We also extract slow scales for space variable n and time variable t.

By inserting $a_c = \frac{2(V'(h) - \lambda)}{1+2\gamma}$, $a = (1 + \varepsilon^2)a_c$ into Eq. (17), one obtains:

$$\varepsilon^4\left[\partial_T R - h_1\partial_X^3 R + h_2\partial_X R^3\right]$$
$$+ \varepsilon^5\left[h_3\partial_X^2 R + h_4\partial_X^4 R + h_5\partial_X^2 R^3\right] = 0. \tag{31}$$

Here, the coefficients h_i are given in Table 1.

In the table, $V' = dV(\Delta x_n)/d\Delta x_n |\Delta x_n = h_c$, $V''' = d^3V(\Delta x_n)/d\Delta x_n^3 |\Delta x_n = h_c$. In order to derive the regularized equation, we make the following transformation:

$$T = \frac{1}{h_1}T', \quad R = \sqrt{\frac{h_1}{h_2}}R' \tag{32}$$

Table 1 Coefficients h_i of the model

h_1		h_2	h_3
$\frac{\lambda V'(1+2\gamma)}{4(V'-\lambda)} + \frac{1+6\gamma}{6} V'$		$\frac{V'''}{6}$	$\frac{1+2\gamma}{2} V'$
h_4		h_5	
$\frac{(1+2\gamma)(2V'-\lambda)}{2(V'-\lambda)} \left(\frac{\lambda V'(1+2\gamma)}{4(V'-\lambda)} + \frac{1+6\gamma}{6} V' \right)$		$\frac{V'''(1+2\gamma)(3V'-2\lambda)}{12(V'-\lambda)}$	
$- \frac{1+14\gamma}{24} V' - \frac{\lambda V'(1+2\gamma)}{12(V'-\lambda)}$			

So the standard mKdV equation with a $O(\varepsilon)$ correction term is showed as follows:

$$\partial_{T'} R' = \partial_X^3 R' - \partial_X R'^3$$
$$- \varepsilon \left[\frac{h_3}{h_1} \partial_X^2 R' + \frac{h_4}{h_1} \partial_X^4 R' + \frac{h_5}{h_2} \partial_X^2 R'^3 \right]. \quad (33)$$

If we ignore the $O(\varepsilon)$, they are just the mKdV equation with a kink solution as the desired Solution:

$$R'_o \left(X, T' \right) = \sqrt{c} \tanh \sqrt{\frac{c}{2}} \left(X - cT' \right). \quad (34)$$

Next, assuming that $R'(X, T') = R'_o(X, T') + \varepsilon R'_1(X, T')$, we take into account the $O(\varepsilon)$ correction. For the purpose of determining the selected value of the velocity c for the kink solution, it is necessary to satisfy the solvability condition

$$\text{As } \left(R'_o, \text{M} \left[R'_o \right] \right) \equiv \int_{-\infty}^{+\infty} \mathrm{d}X' R'_o \text{M} \left[R'_o \right],$$
$$\text{where } \text{M} \left[R'_o \right] = \frac{h_3}{h_1} \partial_X^2 R' + \frac{h_4}{h_1} \partial_X^4 R' + \frac{h_5}{h_2} \partial_X^2 R'^3.$$

We get the general velocity c:

$$c = \frac{5h_2 h_3}{2h_2 h_4 - 3h_1 h_5}. \quad (35)$$

Hence, the general Kink–antikink soliton solution of the headway, from the mKdV equation, is obtained:

$$\Delta x_n(t) = h_c \pm \sqrt{\frac{h_1 c}{h_2} \left(\frac{\tau}{\tau_c} - 1 \right)}$$
$$\times \tanh \sqrt{\frac{c}{2} \left(\frac{\tau}{\tau_c} - 1 \right)}$$
$$\left[n + \left(1 - ch_1 \left(\frac{\tau}{\tau_c} - 1 \right) \right) t \right]. \quad (36)$$

Where $V''' < 0$, this kink soliton solution also represents the coexisting phase and the kink solution (36) is agreed with the solution (25) obtained from the TDGL equation. Thus, the jamming transition can be described by both the TDGL equation with a nontravelling solution and the mKdV equation with a propagating solution.

5 Numerical simulation

Computer simulation is carried out to check the validity of the theoretical results above. Under the periodic boundary condition, the following initial conditions are chosen as follows:

$$\Delta x_n(0) = \Delta x_0 = 4.0, \Delta x_n(1) = \Delta x_0 = 4.0,$$
$$\text{for } n \neq 50, 51, \Delta x_n(1) = 4.0 - 0.5, \text{ for } n = 50,$$
$$\Delta x_n(1) = 4.0 + 0.5, \text{ for } n = 51$$

The total number of cars is $N = 100$ and the sensitivity $a = 1.25$.

Figure 2 shows the space–time evolution of the headway after $t = 10^4$ time steps under the different parameter γ and λ. Pattern (a1) with $\gamma = 0$ and $\lambda = 0$ corresponds to that of the OVM model. In patterns (a1), it can be clearly seen that the traffic flow is very unstable. When a small disturbance is added into the uniform traffic flow, the propagating backward stop-and-go traffic jam appears which is very similar to the mkdV solution. Pattern (b1) with $\gamma = 0$ and $\lambda = 0.15$, we can find that the traffic congestion is becoming relatively stable compared with pattern (a1). Pattern (c1) with $\gamma = 0.2$ and $\lambda = 0$, one can find that the traffic congestion is much less serious in pattern (c1) than in pattern (a1). Pattern (d1) with $\gamma = 0.3$ and $\lambda = 0.2$, we can find that the traffic flow is approaching stability. So it means that the new consideration plays the positive function on the stabilization of traffic flow. As increasing the parameter λ, γ the amplitude of the kink–antikink soliton weakens gradually, which further demonstrates that the new consideration can enhance the stability of traffic flow.

Figure 3 shows the headway profiles obtained at $t = 10,300$ corresponding to panels in Fig. 2, respectively, and from diagrams [(a2), (b2), (c2) and (d2)] we conclude the similar results to Fig. 2. Therefore, the results of simulation are in agreement with those of the theoretical analysis.

(a1) Space-time diagram

(b1) Space-time diagram

(c1) Space-time diagram

(d1) Space-time diagram
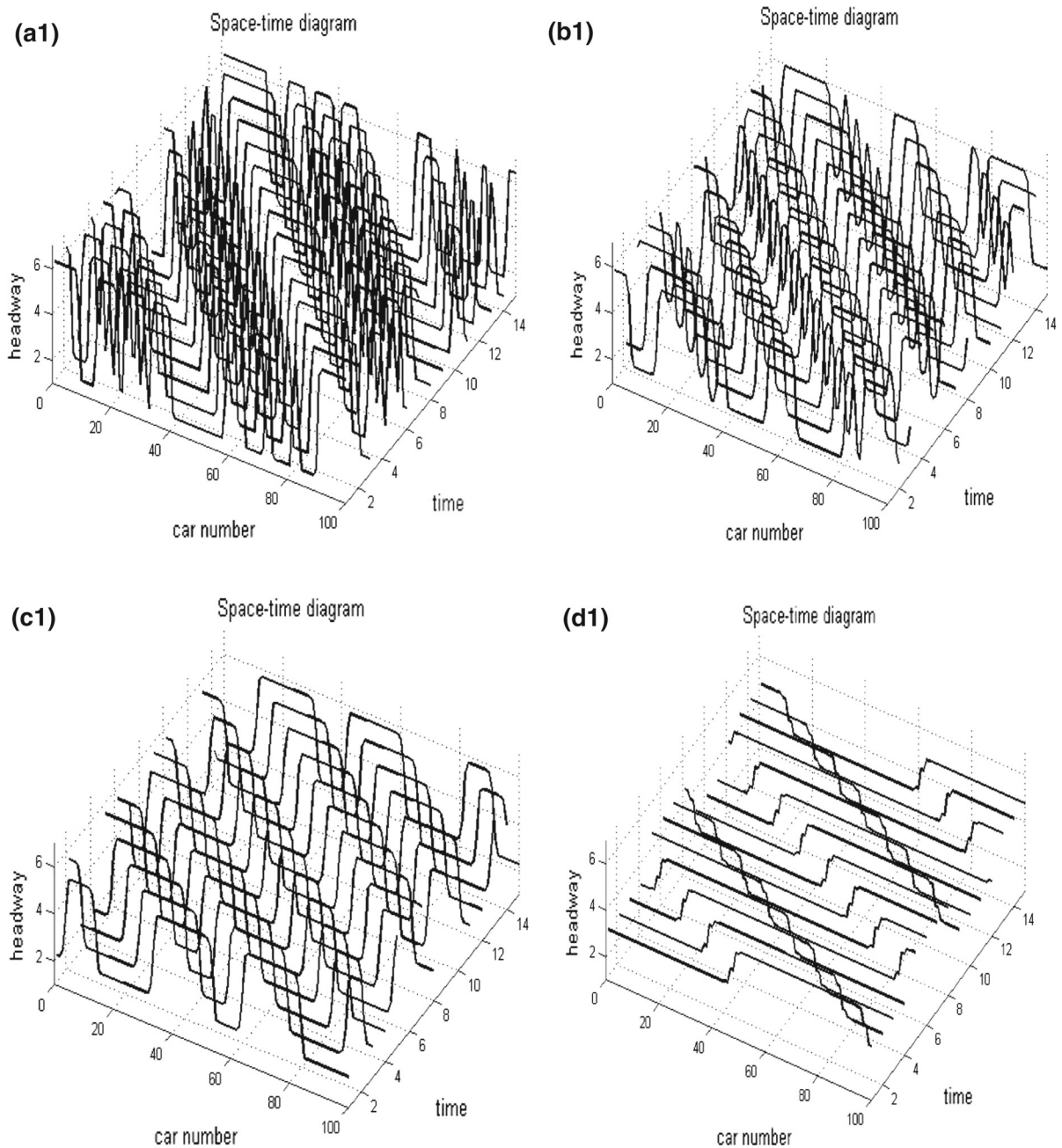
**Fig. 2** Space–time evolution of the headway after $t = 10{,}000$

6 Conclusions

Based on the property of the effect of leading vehicle on current vehicle on a single-lane road, an improved car-following model has been developed to suppress traffic jams. The neutral stability line and the criti-

cal point have been obtained by using the linear stability theory for the OVLM. Furthermore, the TDGL equation has been derived to describe traffic behavior near the critical point by applying the reductive perturbation method. The two corresponding steady-state solutions have been obtained, and the spinodal

Fig. 3 Headway profile at $t = 10{,}300$ under the different value of γ and λ
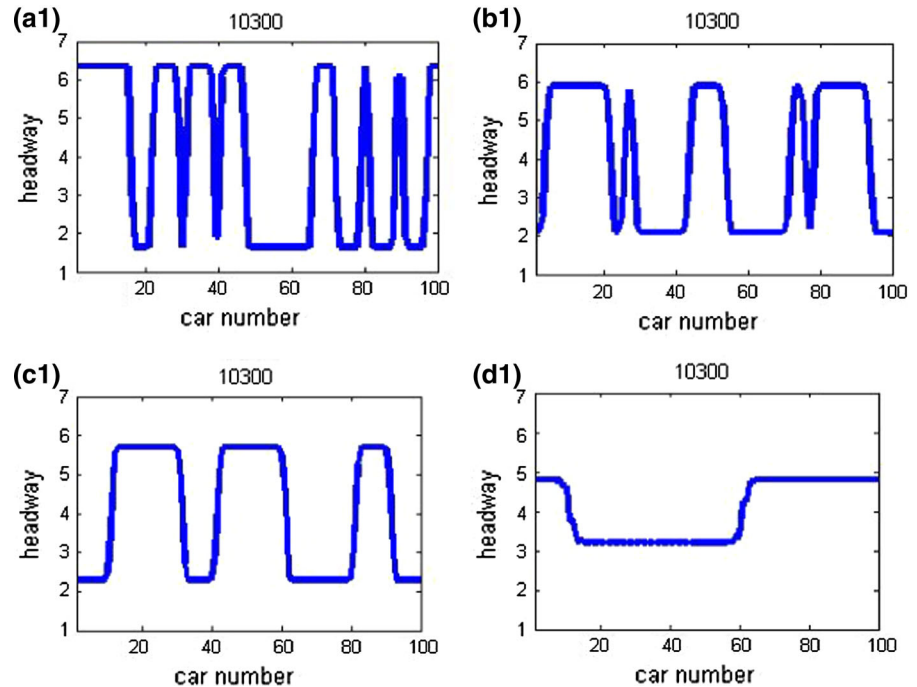
line, the critical point have been calculated from the TDGL equation. The stability condition of the extended model has been obtained, and the results show that the stability of traffic flow is improved by taking the effect of optimal velocity for leading vehicle into account. In addition, we also have derived the mKdV equation from the OVLM. Numerical simulation has shown that the traffic jams are suppressed efficiently through the new model. The analytical results are in good agreement with the simulation results.

References

1. Tang, T.Q., Wang, Y.P., Yang, X.B., Wu, Y.H.: A new car-following model accounting for varying road condition. Nonlinear Dyn. **70**, 1397–1405 (2012)
2. Sharma, S.: Effect of driver's anticipation in a new two-lane lattice model with the consideration of optimal current difference. Nonlinear Dyn. **81**, 991 (2015)
3. Sharma, S.: Lattice hydrodynamic modeling of two-lane traffic flow with timid and aggressive driving behavior. Phys. A **421**, 401 (2015)
4. Li, Z.P., Liu, F.Q., Sun, J.: A lattice model with consideration of preceding mixture traffic information. Chin. Phys. B **20**, 088901 (2011)
5. Peng, G.H.: A driver's memory lattice model of traffic flow and its numerical simulation. Nonlinear Dyn. **67**, 1811–1815 (2012)
6. Redhu, P., Gupta, A.K.: Effect of forward looking sites on a multi-phase lattice hydrodynamic model. Phys. A **445**, 150 (2016)
7. Redhu, P., Gupta, A.K.: Delayed-feedback control in a Lattice hydrodynamic model. Commun. Nonlinear Sci. Numer. Simul. **27**, 263 (2015)
8. Kang, Y.R., Sun, D.H.: Lattice hydrodynamic traffic flow model with explicit driver's physical delay. Nonlinear Dyn. **71**, 531–537 (2013)
9. Gupta, A.K., Sharma, S., Redhu, P.: Effect of multi-phase optimal velocity function on jamming transition in a lattice hydrodynamic model with passing. Nonlinear Dyn. **80**, 1091 (2015)
10. Gupta, A.K., Sharma, S., Redhu, P.: Analyses of lattice traffic flow model on a gradient highway. Commun. Theor. Phys. **62**, 393 (2014)
11. Li, Y.F., Sun, D.H., Liu, W.N., Zhang, M., Zhao, M., Liao, X.Y., Tang, L.: Modeling and simulation for microscopic traffic flow based on multiple headway, velocity and acceleration difference. Nonlinear Dyn. **66**, 15–28 (2011)
12. Peng, G.H., Cai, X.H., Liu, C.Q., Tuo, M.X.: A new lattice model of traffic flow with the anticipation effect of potential lane changing. Phys. Lett. A **376**, 447–451 (2012)

13. Zhou, T., Sun, D.H., Kang, Y.R., Li, H.M., Tian, C.: A new car-following model with consideration of the prevision driving behavior. Commun. Nonlinear Sci. Numer. Simul. **19**, 3820–3826 (2014)

14. Moussa, N., Daoudia, A.K.: Numerical study of two classes of cellular automaton models for traffic flow on a two-lane roadway. Eur. Phys. B **31**, 413–420 (2003)

15. Zheng, L.J., Tian, C., Sun, D.H., Liu, W.N.: A new car-following model with consideration of anticipation driving behavior. Nonlinear Dyn. **70**, 1205–1211 (2012)

16. Tang, T.Q., Shi, W.F., Shang, H.Y., Wang, Y.P.: A new car-following model with consideration of inter-vehicle communication. Nonlinear Dyn. **76**, 2017–2023 (2014)

17. Pipes, L.A.: An operational analysis of traffic dynamic. J. Appl. Phys. **24**, 274–281 (1953)

18. Bagdadi, O., Varhelyi, A.: Development of a method for detecting jerks in safety critical events. Accid. Anal. Prev. **50**, 83–91 (2013)

19. Yu, S.W., Shi, Z.K.: An extended car-following model considering vehicular gap fluctuation. Measurement **70**, 137–147 (2015)

20. Newell, G.F.: Nonlinear effects in the dynamics of car following. Oper. Res. **9**, 209–229 (1961)

21. Tang, T.Q., Huang, H.J., Shang, H.Y.: A new macro model for traffic flow with the onsideration of the driver's forecast effect. Phys. Lett. A **374**, 1668–1672 (2010)

22. Jiang, R., Wu, Q.S., Jia, B.: Intermittent unstable structures induced by incessant constant disturbances in the full velocity difference car-following model. Phys. D **237**, 467–474 (2008)

23. Bando, M., Haseba, K., Nakayama, A., Shibata, A., Sugiyama, Y.: Dynamical model of traffic congestion and numerical simulation. Phys. Rev. E **51**, 1035–1042 (1995)

24. Helbing, D., Tilch, B.: Generalized force model of traffic dynamic. Phys. Rev. E **58**, 133–138 (1998)

25. Jiang, R., Wu, Q.S., Zhu, Z.J.: Full velocity difference model for a car-following theory. Phys. Rev. E **64**, 017101 (2001)

26. Ge, H.X., Cheng, R.J., Li, Z.P.: Two velocity difference model for a car following theory. Phys. A **387**, 5239–5245 (2008)

27. Ge, J.L., Orosz, G.: Dynamics of connected vehicle systems with delayed acceleration feedback. Transp. Res. C **46**, 46–64 (2014)

28. Yu, S.W., Shi, Z.K.: Dynamics of connected cruise control systems considering velocity changes with memory feedback. Measurement **64**, 34–48 (2015)

29. Yu, S.W., Shi, Z.K.: An extended car-following model at signalized intersections. Phys. A **407**, 152–159 (2014)

30. Yu, S.W., Shi, Z.K.: An improved car-following model with two preceding cars' average speed. Int. J. Mod. Phys. C **26**, 1550094 (2015)

31. Peng, G.H., Sun, D.H.: A dynamical model of car-following with the consideration of the multiple information of preceding cars. Phys. Lett. A **374**, 1694–1698 (2010)

32. Tang, T.Q., Li, C.Y., Huang, H.J., Shang, H.Y.: A new fundamental diagram theory with the individual difference of the drivers' perception ability. Nonlinear Dyn. **67**, 2255–2265 (2012)

33. Li, Z.P., Li, W.Z., Xu, S.Z., Qian, Y.Q.: Analysis of vehicles's self-stabilizing effect in an extended optimal velocity model by utilizing historical velocity in an environment of intelligent transportation system. Nonlinear Dyn. **80**, 529–540 (2015)

34. Zhu, W.X., Yu, R.L.: Nonlinear analysis of traffic flow on a gradient highway. Phys. A **391**, 954 (2012)

35. Yu, S.W., Shi, Z.K.: An improved car-following model considering headway changes with memory. Phys. A **421**, 1–14 (2015)

36. Lv, F., Zhu, H.B., Ge, H.X.: TDGL and mKdv equations for car-following model considering driver's anticipation. Nonlinear Dyn. **77**, 1245–1250 (2014)

37. Nagatani, T.: Jamming transition in the lattice models of traffic. Phys. Rev. E **59**, 4857–4864 (1999)

38. Nagatani, T.: Thermodynamic theory for the jamming transition in traffic flow. Phys. Rev. E **58**, 4271–4276 (1998)

39. Nagatani, T.: TDGL and mKdV equation for jamming transition in the lattice models of traffic. Phys. A **264**, 581–592 (1999)

40. Nagatani, T.: Jamming transitions and the modified Korteweg–de Vries equation in a two-lane traffic flow. Phys. A **265**, 297–310 (1999)